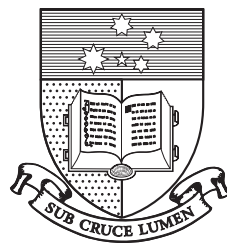


# Computation of Axial and Near-Axial Flow Over a Long Circular Cylinder

A thesis for the degree of  
Doctor of Philosophy

Milton J. Woods  
June 2006

Presented to the  
School of Mechanical Engineering  
The University of Adelaide  
Australia



# Contents

<b>Contents</b>	<b>i</b>
<b>List of Figures</b>	<b>v</b>
<b>List of Tables</b>	<b>ix</b>
<b>Abstract</b>	<b>xi</b>
<b>Acknowledgments</b>	<b>xiii</b>
<b>Declaration</b>	<b>xv</b>
<b>1 Introduction</b>	<b>1</b>
1.1 Axisymmetric Flow Regimes . . . . .	2
1.2 Numerical Simulation . . . . .	3
1.3 Near-Axial Flow . . . . .	4
1.4 Scope of the Present Work . . . . .	5
<b>2 Simulation Methodology</b>	<b>7</b>
2.1 Computational Model . . . . .	7
2.2 Governing Equations . . . . .	11
2.2.1 Definition of Vorticity . . . . .	11
2.2.2 Divergence Specifications . . . . .	11
2.2.3 Vorticity Transport Equation . . . . .	12
2.2.4 Potential Flow . . . . .	14
2.3 Spectral Formulation . . . . .	14
2.3.1 Fourier Series . . . . .	14
2.3.2 Chebyshev Series . . . . .	16
2.4 Time Advancement . . . . .	18
2.4.1 Uncoupling the Viscous Operators . . . . .	18
2.4.2 Time-Stepping Scheme . . . . .	20

2.4.3	Evaluation of Non-Linear Term . . . . .	21
2.4.4	Vorticity Boundary Conditions . . . . .	22
2.4.5	Azimuthal-Axial-Mean Vorticity . . . . .	24
2.5	Velocity Calculation . . . . .	25
2.5.1	Background . . . . .	25
2.5.2	Velocity Decomposition . . . . .	26
2.5.3	Boundary Conditions . . . . .	26
2.5.4	Free-Stream Velocity . . . . .	27
2.5.5	Vortical Velocity . . . . .	28
2.5.6	General Solutions for Potential Flow . . . . .	30
2.5.7	Particular Solutions for Potential Flow . . . . .	32
2.6	Pressure Calculation . . . . .	37
2.7	Numerical Methods . . . . .	38
2.7.1	Galerkin Method . . . . .	38
2.7.2	Faddeev-Faddeeva Factorisation . . . . .	41
2.7.3	Bessel Function Calculation . . . . .	43
2.8	Summary . . . . .	44
<b>3</b>	<b>Computational Considerations</b>	<b>47</b>
3.1	Code Development and Verification . . . . .	47
3.2	Specification of Flow Parameters . . . . .	48
3.3	Geometrical and Temporal Parameters . . . . .	49
3.4	Mesh Validation . . . . .	54
3.5	Statistical Steadiness . . . . .	59
3.6	Summary . . . . .	61
<b>4</b>	<b>Velocity Statistics</b>	<b>63</b>
4.1	Mean Velocity . . . . .	63
4.2	Reynolds Shear-Stress . . . . .	74
4.3	Turbulence Intensities . . . . .	77
4.4	Turbulence Kinetic Energy Budget . . . . .	81
4.5	Higher-Order Moments . . . . .	86
4.6	Quadrant Analysis . . . . .	92
4.7	Vorticity Fluctuations . . . . .	92
4.8	Summary and Conclusions . . . . .	98
<b>5</b>	<b>Pressure Statistics</b>	<b>103</b>
5.1	Moments about the Mean . . . . .	103

---

5.2	Green's Function Analysis . . . . .	107
5.3	Pressure-Source Fluctuations . . . . .	109
5.4	Spatial Spectra of Wall-Pressure . . . . .	113
5.5	Temporal Spectra of Wall-Pressure . . . . .	115
5.6	Convection Velocity . . . . .	121
5.7	Root-Mean-Square Wall-Pressure . . . . .	122
5.8	Summary and Conclusions . . . . .	128
<b>6</b>	<b>Flow Structure</b>	<b>133</b>
6.1	Instantaneous Flow Fields . . . . .	134
6.2	Two-point Correlations . . . . .	157
6.3	Conditional Averages . . . . .	163
6.4	Summary and Conclusions . . . . .	167
<b>7</b>	<b>Near-Axial Flow</b>	<b>171</b>
7.1	Turbulent Near-Axial Flow . . . . .	171
7.1.1	Computational Considerations . . . . .	171
7.1.2	Mean Flow . . . . .	172
7.1.3	Turbulence Statistics . . . . .	176
7.1.4	Instantaneous Flow Fields . . . . .	181
7.2	Vortex-Shedding in Near-Axial Flow . . . . .	188
7.3	Summary and Conclusions . . . . .	193
<b>8</b>	<b>Research Findings</b>	<b>197</b>
8.1	Introduction . . . . .	197
8.2	Simulation Boundary Conditions . . . . .	198
8.3	Turbulent Cross-Flow Events . . . . .	199
8.4	Mean Velocity Profiles . . . . .	201
8.5	Velocity-Scale for Axisymmetric Flow . . . . .	202
8.6	Temporal Spectra of Wall-Pressure . . . . .	204
8.7	Turbulent Near-Axial Flow . . . . .	206
8.8	Vortex-Shedding in Near-Axial Flow . . . . .	207
8.9	Future Work . . . . .	208
	<b>Nomenclature</b>	<b>211</b>
	<b>References</b>	<b>215</b>
	<b>Publications</b>	<b>221</b>

# List of Figures

2.1	Schematic diagram of the computational model. . . . .	9
2.2	Modified Bessel functions $I_n[x]$ and $K_n[x]$ for positive $x$ and integer $n$ . . . . .	32
3.1	Azimuthal spectra of the axial velocity component. . . . .	56
3.2	Axial spectra of the axial velocity component. . . . .	57
3.3	Axial two-point correlations of axial velocity fluctuations. . . . .	58
3.4	Axial pressure-gradient at the statistically-steady state. . . . .	60
3.5	Total shear-stress normalised by wall-shear-stress. . . . .	62
4.1	Mean velocity profiles in flat-plate wall units. . . . .	69
4.2	Mean velocity profiles in axisymmetric wall units. . . . .	71
4.3	Ratio $V_\infty/u_\tau$ as a function of both $Re_a$ and $\delta/a$ . . . . .	72
4.4	Velocity-defect profiles for cylinder and plane-channel simulations. . . . .	73
4.5	Reynolds shear-stress in wall units. . . . .	75
4.6	Reynolds shear-stress as functions of $y/h$ scaled with $u_\tau$ and $u_{\tau c}$ . . . . .	76
4.7	RMS velocity fluctuations in wall units. . . . .	78
4.8	RMS velocity fluctuations as functions of $y/h$ scaled with $u_{\tau c}$ . . . . .	80
4.9	Terms of turbulence kinetic energy budget: production and velocity pressure-gradient. . . . .	83
4.10	Terms of turbulence kinetic energy budget: turbulent transport and viscous diffusion. . . . .	84
4.11	Terms of turbulence kinetic energy budget: viscous dissipation and total rate of change. . . . .	85
4.12	Example time-series of axial velocity fluctuations. . . . .	87
4.13	Skewness profiles of velocity fluctuations. . . . .	88
4.14	Flatness profiles of velocity fluctuations. . . . .	89
4.15	Fraction of mean Reynolds shear-stress contributed by each quadrant as a function of $y^+$ . . . . .	93

4.16	Fraction of mean Reynolds shear-stress contributed by each quadrant as a function of threshold. . . . .	94
4.17	RMS vorticity fluctuations in wall units. . . . .	95
4.18	RMS vorticity fluctuations as functions of $y/h$ . . . . .	97
5.1	Profiles of RMS pressure fluctuations. . . . .	105
5.2	Skewness and flatness profiles of pressure fluctuations. . . . .	106
5.3	Wall-pressure due to a point source of unit strength as a function of source position and axial wave-number. . . . .	108
5.4	RMS fluctuations of pressure-source terms. . . . .	110
5.5	RMS fluctuations of total pressure-source. . . . .	112
5.6	Spatial wave-number spectra of wall-pressure fluctuations. . . . .	114
5.7	Temporal spectra of wall-pressure in mid-frequency form. . . . .	118
5.8	Temporal spectra of wall-pressure in high-frequency form. . . . .	120
5.9	Estimated temporal spectra of wall-pressure obtained from spatial spectra using Taylor's hypothesis. . . . .	123
5.10	RMS wall-pressure fluctuations as a function of $\delta^+$ . . . . .	124
5.11	RMS wall-pressure fluctuations as a function of $L_p^+$ . . . . .	127
6.1	Instantaneous axial velocity fluctuations in plane $z^+ = 1250$ for $Re_a = 2600$ , $b/a = 6$ . . . . .	136
6.2	Instantaneous axial velocity fluctuations in plane $z^+ = 1250$ for $Re_a = 311$ , $b/a = 41$ . . . . .	137
6.3	Instantaneous axial velocity fluctuations in plane $X = 0$ for $Re_a = 2600$ , $b/a = 6$ . . . . .	138
6.4	Instantaneous axial velocity fluctuations in plane $X = 0$ for $Re_a = 311$ , $b/a = 41$ . . . . .	139
6.5	Instantaneous axial velocity fluctuations at $y^+ = 15$ . . . . .	140
6.6	Instantaneous radial velocity in plane $z^+ = 1250$ for $Re_a = 2600$ , $b/a = 6$ . . . . .	142
6.7	Instantaneous radial velocity in plane $z^+ = 1250$ for $Re_a = 311$ , $b/a = 41$ . . . . .	143
6.8	Instantaneous radial velocity in plane $X = 0$ for $Re_a = 2600$ , $b/a = 6$ . . . . .	144
6.9	Instantaneous radial velocity in plane $X = 0$ for $Re_a = 311$ , $b/a = 41$ . . . . .	145
6.10	Instantaneous radial velocity at $y^+ = 15$ . . . . .	146
6.11	Instantaneous azimuthal velocity in plane $z^+ = 1250$ for $Re_a = 2600$ , $b/a = 6$ . . . . .	148

6.12	Instantaneous azimuthal velocity in plane $z^+ = 1250$ for $Re_a = 311$ , $b/a = 41$ . . . . .	149
6.13	Instantaneous azimuthal velocity in plane $X = 0$ for $Re_a = 2600$ , $b/a = 6$ . . . . .	150
6.14	Instantaneous azimuthal velocity in plane $X = 0$ for $Re_a = 311$ , $b/a = 41$ . . . . .	151
6.15	Instantaneous azimuthal velocity at $y^+ = 15$ . . . . .	152
6.16	Instantaneous axial vorticity at $y^+ = 15$ . . . . .	153
6.17	Instantaneous radial vorticity at $y^+ = 15$ . . . . .	154
6.18	Instantaneous azimuthal vorticity fluctuations at $y^+ = 15$ . . . . .	155
6.19	Instantaneous wall-pressure fluctuations. . . . .	156
6.20	Streamwise (axial) two-point velocity correlations. . . . .	158
6.21	Spanwise (azimuthal) two-point velocity correlations. . . . .	160
6.22	Two-point correlations of wall-pressure fluctuations. . . . .	162
6.23	Visualisation of conditionally averaged burst event. . . . .	164
6.24	Conditionally averaged velocity in $r$ - $z$ planes. . . . .	166
7.1	Contours of mean velocity for turbulent near-axial flow. . . . .	174
7.2	Mean velocity profiles in wall units for turbulent near-axial flow. . . . .	176
7.3	Reynolds shear-stress for $\beta = 0.5^\circ$ , $Re_a = 674$ , $\delta^*/a = 0.984$ . . . . .	177
7.4	RMS velocity fluctuations for $\beta = 0.5^\circ$ , $Re_a = 674$ , $\delta^*/a = 0.984$ . . . . .	178
7.5	RMS vorticity fluctuations for $\beta = 0.5^\circ$ , $Re_a = 674$ , $\delta^*/a = 0.984$ . . . . .	179
7.6	Profiles of RMS pressure for $\beta = 0.5^\circ$ , $Re_a = 674$ , $\delta^*/a = 0.984$ . . . . .	180
7.7	Instantaneous velocity fluctuations in plane $z^+ = 1250$ for $\beta = 0.5^\circ$ , $Re_a = 674$ , $\delta^*/a = 0.984$ . . . . .	182
7.8	Instantaneous axial velocity fluctuations in plane $Y = 0$ for $\beta = 0.5^\circ$ , $Re_a = 674$ , $\delta^*/a = 0.984$ . . . . .	183
7.9	Instantaneous radial velocity fluctuations in plane $Y = 0$ for $\beta = 0.5^\circ$ , $Re_a = 674$ , $\delta^*/a = 0.984$ . . . . .	184
7.10	Instantaneous azimuthal velocity fluctuations in plane $Y = 0$ for $\beta = 0.5^\circ$ , $Re_a = 674$ , $\delta^*/a = 0.984$ . . . . .	185
7.11	Instantaneous velocity fluctuations at $y^+ = 15$ for $\beta = 0.5^\circ$ , $Re_a =$ $674$ , $\delta^*/a = 0.984$ . . . . .	186
7.12	Instantaneous wall-pressure fluctuations for $\beta = 0.5^\circ$ , $Re_a = 674$ , $\delta^*/a = 0.984$ . . . . .	187
7.13	Axial velocity in vortex-shedding near-axial flow as a function of time or axial position. . . . .	189

---

7.14	Instantaneous velocity for vortex-shedding near-axial flow ( $\beta = 3^\circ$ , $Re_a = 311, b/a = 21$ ) . . . . .	191
7.15	Instantaneous vorticity for vortex-shedding near-axial flow ( $\beta = 3^\circ$ , $Re_a = 311, b/a = 21$ ) . . . . .	192
7.16	Instantaneous wall-pressure for vortex-shedding near-axial flow ( $\beta =$ $3^\circ, Re_a = 311, b/a = 21$ ) . . . . .	194



# List of Tables

2.1	Coefficients for stiffly-stable integration schemes up to third order. . .	21
3.1	Grid geometry parameters . . . . .	50
3.2	Grid resolution in mean-flow wall units. . . . .	50
3.3	Temporal averaging intervals . . . . .	53
3.4	Temporal resolution of time-series . . . . .	53
4.1	Mean-flow parameters for present simulations. . . . .	64
4.2	Mean-flow parameters for reference data. . . . .	66
4.3	Integral thickness parameters for present simulations. . . . .	67
4.4	Integral thickness parameters for reference data. . . . .	68
4.5	Quadrants of the Reynolds shear-stress. . . . .	92
5.1	Frequency ranges and spectral forms for wall-pressure in planar boundary layers. . . . .	116
5.2	Frequency ranges and spectral forms for wall-pressure in transversely curved boundary layers. . . . .	130
7.1	Mean velocity parameters for turbulent near-axial flow . . . . .	173

# Abstract

A direct numerical simulation study has been conducted to examine the flow that develops on long circular cylinders that are aligned, or nearly aligned, with the free-stream. Results are presented for turbulent boundary layers and vortex-shedding yawed flow. Although flows of these types occur in a range of engineering applications, they remain relatively unexplored compared with flat-plate flow.

The numerical scheme employed for solution of the governing Navier-Stokes equations is similar to that used in some previously published simulations, but here rather different boundary conditions are adopted. At the outer edge of the cylindrical computational domain, the imposed boundary conditions confine the vorticity field within a finite radius while allowing the continuous velocity field to converge to the free-stream velocity at large distances from the cylinder.

Axial flows are considered with radius Reynolds numbers in the range 311 to 20800, ratios of boundary layer thickness to cylinder radius in the range 0.15 to 27.5, and boundary layer thicknesses of between 160 and 800 viscous units ( $\nu/u_\tau$ ). The mean-flow and turbulence statistics for axisymmetric boundary layers are found to differ significantly from flat-plate results when the boundary layer is strongly curved, that is when the boundary layer is thick in relation to the cylinder radius. The effects of curvature are mainly observed in the outer flow except when the cylinder radius in viscous units is small. Particular attention is given to the assessment of similarity scaling relations for the mean velocity profile, velocity fluctuation statistics and temporal wall-pressure spectra.

Structural features of axisymmetric turbulence are examined by inspection of instantaneous flow fields, correlation functions and conditionally-averaged flow structures. In very thick boundary layers on thin cylinders, the simulations reveal evidence of large-scale fluid motion across the cylinder, although the mechanisms of turbulence generation do not appear to be significantly different from those in flat-plate flow.

Simulations of turbulence in near-axial flow over cylinders are considered with radius Reynolds numbers up to 674 and yaw angles up to 0.5 degrees. No previous

flow simulations of this kind are reported in the literature. The mean-flow and turbulence statistics are found to depart rapidly from axisymmetry as the yaw angle increases. The quality of the calculated results suggests that the computational procedure is suitable for use in a more comprehensive investigation of near-axial flow over cylinders.

For cylinders inclined at sufficiently large yaw angles to the free-stream, turbulent boundary layer flow gives way to oblique vortex-shedding from the cylinder. Simulated flow fields corresponding to a radius Reynolds number of 311 and a yaw angle of 3 degrees are examined to reveal the three-dimensional structure of the flow. The results suggest that the oscillating flow fields in the cylinder wake have the character of a wave travelling in the axial direction at the same speed as the axial component of the free-stream.

# Acknowledgments

The work leading to this thesis has been assisted by a number of organisations and individuals, whose contributions are gratefully acknowledged.

Financial support for the current project has been provided by the Australian Research Council (ARC), in the form of an Australian Postgraduate Award (Industry), with additional funding provided by Thales Underwater Systems Pty. Ltd. The project is a continuation of research funded by an ARC Cooperative Research Grant in conjunction with Australia Sonar Systems Pty. Ltd., which subsequently became part of Thales Underwater Systems Pty. Ltd.

The project has been supervised by Dr. M. K. (Max) Bull, Dr. Bassam Dally and Prof. R. E. (Sam) Luxton in the School of Mechanical Engineering. Their advice and criticism has led me to work to the best of my ability. I also appreciate the assistance given by Dr. Allan Carpenter, who played the role of project liaison at Thales Underwater Systems Pty. Ltd.

The computational resources used for the project have been provided by several organisations. In the early stages of the project, I learnt the fundamentals of parallel programming on the CM-5 supercomputer operated by the South Australian Centre for Parallel Computing (SACPC). A substantial grant of processing time, some 45000 CPU-hours in total, has been provided by the Australian Partnership for Advanced Computing (APAC) through the Merit Allocation Scheme. The bulk of the results presented in this thesis have been generated using several CPU-decades of processing time on supercomputers operated by the South Australian Partnership for Advanced Computing (SAPAC). Special thanks go to the system administrators, Grant Ward and Patrick Fitzhenry, whose friendly and dedicated assistance helped me to get work done with the minimum of delay. I would also like to thank Dr. Francis Vaughan, who has given support and advice on computational aspects of the current project since the days of the CM-5.

I thank my fellow postgraduate students, who have helped me in very many ways, and with whom I have shared some great times. While there are too many

people to mention individually here, I offer my most sincere thanks to Eyad Hassan, Antoni Blazewicz and Federico Berera for their friendship over many years.

It needs to be said that the staff of the School of Mechanical Engineering work with real dedication to provide a rich educational environment for their students. I would particularly like to thank George Osborne, Dr. Richard Kelso and Dr. Anthony Zander for the interest they have shown in me and my work. Many thanks also go to Billy Constantine for his great work as the Computing Officer.

I have greatly appreciated the patience and understanding of my family and friends throughout the duration of my postgraduate research program and particularly while I have been writing this thesis.

Finally, I wish to thank my wife Robyn, without whose encouragement and support I could never have completed the present work.

# Declaration

This work contains no material which has been accepted for the award of any other degree or diploma in any university or other tertiary institution and, to the best of my knowledge and belief, contains no material previously published or written by another person, except where due reference has been made in the text.

I give consent to this copy of my thesis, when deposited in the University Library, being available for loan and photocopying.

Milton J. Woods

June 28, 2006